Journal of Ocean University of China (Oceanic and Coastal Sea Research)
ISSN 1672-5182, April 30, 2006, Vol.5, No.2, pp.123-131
http://www.ouc.edu.cn/xbywb/
E-mail: xbywb@mail.ouc.edu.cn

Phytoplankton Assemblage of Yangtze River Estuary and the Adjacent East China Sea in Summer, 2004

LUAN Qingshan[1),2)], SUN Jun[2),*], SHEN Zhiliang[2)], SONG Shuqun[2)], and WANG Min[1)]

1) *College of Marine Life Science, Ocean University of China, Qingdao* 266003, *P. R. China*
2) *Key Laboratory of Marine Ecology & Environmental Science, Institute of Oceanology, Chinese Academy of Sciences, Qingdao* 266071, *P. R. China*

(Received July 21, 2005; accepted January 25, 2006)

Abstract A cruise was conducted from late August to early September 2004 with the intention of obtaining an interdisciplinary understanding of the Yangtze River Estuary including the biological, chemical and physical subjects. Water sample analysis indicated that total phytoplankton species richness was 137. Of them 81 were found in Bacillariophyta and 48 in Pyrrophyta, accounting for 59.1% and 35.0% respectively. The average cell abundance of surface water samples was 8.8×10^4 cells L^{-1}, with the maximum, 102.9×10^4 cells L^{-1}, encountered in the area (31.75°N, 122.33°E) and the minimum, 0.2×10^4 cells L^{-1}, in (30.75°N, 122.17°E). The dominant species at most stations were *Skeletonema costatum* and *Proboscia alata* f. *gracillima* with the dominance of 0.35 and 0.27. Vertical distribution analysis indicated that obvious stratification of cell abundance and dominant species was found in the representative stations of 5, 18 and 33. Shannon-Wiener index and evenness of phytoplankton assemblage presented negative correlation with the cell abundance, with the optimum appearing in (30.75°N, 122.67°E). According to the PCA analysis of the environmental variables, elevated nutrients of nitrate, silicate and phosphate through river discharge were mainly responsible for the phytoplankton bloom in this area.

Key words Yangtze River Estuary; phytoplankton; nutrients; eutrophication; *Skeletonema costatum*; *Proboscia alata* f. *gracillima*

1 Introduction

Phytoplankton play an important role in primary production through the formation of chlorophyll *a* in the ocean using the solar energy. They are important biological mediators of carbon turnover in pelagic ecosystems. Through photosynthesis, they transform inorganic carbon into particulate and dissolving organic compounds that in turn are either metabolised in seawater column or precipitated by sinking (particulate) or participating in water movement (both dissolving and particulate). Thus, their activity sets the upper limit of carbon entry into food web.

The Yangtze River Estuary (YRE) is a mesotidal coastal estuary bordering the highly urbanized and industrialized city Shanghai, China. The Yangtze River basin encompasses a surface acreage of 1.8×10^6 km^2, and its freshwater discharged into the East China Sea (ECS) reaches 9.32×10^{11} m^3, with 4.68×10^8 t sediment, 6.3×10^6 t nitrate, 0.13×10^6 t phosphate, and 20.4×10^6 t dissolved silica each year (Chen *et al.*, 1989; Shen *et al.*, 1992). Five water masses influence the characteristics of phytoplankton community structure, according to the salinities and geographical distributions of the survey area. They are Yangtze River fresh water with a salinity no higher than 5, Yangtze River diluted water with the salinity between 5 – 31, underlayer water of the Yellow Sea with a salinity lower than 31.8, Taiwan Warm Current and mixed water of the Yellow Sea and ECS with a salinity higher than 32. The Yangtze River diluted water extends toward the south along the coast during winter, and the northeast during summer. The strength and area of the latter are obviously larger than those of the former, and the latter constitutes the main Yang-tze River plume (Ning *et al.*, 1988; Zhu *et al.*, 2005).

A sharp salinity gradient in the YRE results in highly diversified composition of phytoplankton species compared with that in other seas. Although phytoplankton assemblage is determined by many factors (biological, chemical and hydrological variables), enriched nutrients in YRE are presumably the main reasons for the increase of phytoplankton biomass (derived from chlorophyll *a*) in the estuary. The fluctuation of inorganic nutrient content has the potential of forming the nitrate or phosphate limitation of the phytoplankton growth. Nutrients decrease in the YRE with the distance from the river mouth. Irradiance becomes the primary limiting factor in the mouth area

* Corresponding author. Tel: 0086-532-82898647
E-mail: sunjun@ms.qdio.ac.cn

because of the very rich suspending solids. Co-limitation of phosphate and nitrate plays an important role in the middle of the dilution zone, while in the offshore nitrate is the main limiting factor (Pu *et al.*, 2000, 2001; Zhao *et al.*, 2004).

The purpose of this study is to describe the characteristics of phytoplankton community structure caused by species composition, phytoplankton diversity index and spatial distribution of cell abundance, and to clarify the relationship between the nutrient pulsing of YRE and the phytoplankton biomass, in order to identify the principal environmental factors influencing the phytoplankton growth and production that have been scarcely studied previously.

2 Materials and Methods

2.1 Study Area

A multidisciplinary investigation on the marine ecosystem of YRE and the adjacent ECS was carried out from August 28 to September 6, 2004. The area and the sampling stations are shown in Fig.1. This area is located between 30.5°– 32.5°N and 121.0°– 123.5°E. Regions Ⅰ, Ⅱ and Ⅲ are estuary fresh water, diluted water and highi salty pelagic water respectively.

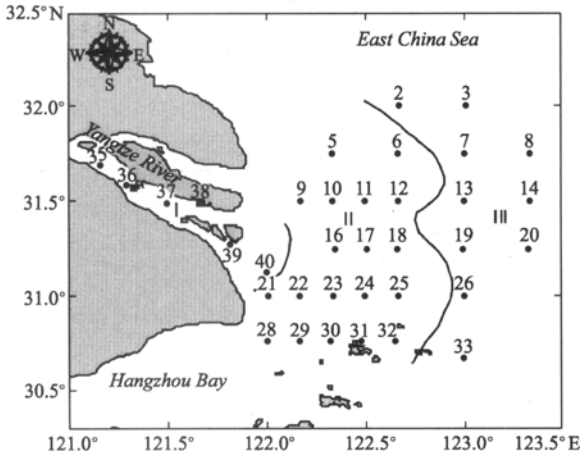

Fig.1 The phytoplankton sampling stations in YRE and ECS, China.

2.2 Phytoplankton Samples

Phytoplankton water samples were collected using 12 L Niskin bottles at the depths of 0 m, 5 m, 10 m, 20 m, 30 m and sea floor. The samples were fixed with buffered formaldehyde at a final concentration of about 1.0% in 250 mL PE bottles. Cell enumeration and species identification were performed by using an inverted microscope (American Optical Ltd.) at × 100 – 400 magnification after sedimentation for 24 h in 25 mL Utermöhl chambers (Utermöhl, 1958). Phytoplankton were identified to the lowest taxon (genus or species) as possible as we can and accordingly counted (Tomas, 1997; Yamaji, 1991). The error sources of Utermöhl method were corrected by the mean square estimate calculation with finite population corrections using the following equation (Sun *et al.*, 2002a)

$$MS_1 = \overline{x}_{st}(v_{st}/v_4)[(v_3 - n_4 \cdot v_4)/v_3] + n_4 \cdot \overline{x}_{st}(v_{st}/v_3)[(v_2 - n_3 \cdot v_3)/v_2] + n_3 \cdot n_4 \cdot \overline{x}_{st}(v_{st}/v_2)[(v_2 - v_3)/v_2] + n_2 \cdot n_3 \cdot n_4 \cdot \overline{x}_{st}(v_{st}/v_1)[(v_1 - v_2)/v_1],$$

where MS_1 is the mean square at level one; n_1, n_2, n_3 and n_4 are the number of primary samples, the number of secondary subsamples per primary sample, the number of tertiary subsamples per secondary subsample, and the number of quartus subsamples per tertiary subsample; v_1, v_2, v_3 and v_4 are volumes of the primary sample, secondary subsample, tertiary subsample, and quartus subsample; $\overline{x}_{st}$ is sample mean; and v_{st} is standard volume (cells L^{-1}).

2.3 Community Structure Analysis

Phytoplankton diversity was calculated using a bio-related version of Shannon-Wiener index (Shannon and Wiener, 1949) as follows:

$$H' = -\sum_{i=1}^{S} P_i \log_2 P_i,$$

where P_i is relative species biomass and i and S are the number of species. Evenness was calculated using H' (Pielou, 1969) as follows:

$$J = \frac{H'}{\log_2 S},$$

where H' is the Shannon-Wiener index in a sample and S is the number of species in a sample. Phytoplankton dominance in this area is calculated using the following formula:

$$Y = \frac{n_i}{N} f_i,$$

where n_i is the number of the species individuals, f_i is the frequency of species occurring in a sample and N is the total number of individuals.

3 Results

3.1 Hydrology of Study Area

Hydrological characteristics of YRE investigated during the cruise included temperature, salinity, dissolved oxygen (DO), pH and nutrient salts. Surface temperature and salinity distribution were shown in Fig.2. The salinity of YRE was strongly influenced by various water masses, ranging from 7.36 to 24.20 in the diluted area (Ⅱ) and from 24.61 to 34.35 in the

eastern pelagic area (Ⅲ). However, changes of the temperature, pH and DO in surface water were not sharp, *i. e.*, 26.70℃ ± 0.83℃, 8.05 mg L^{-1} ± 0.10 mg L^{-1} and 6.74 mg L^{-1} ± 0.89 mg L^{-1} respectively on average. NO_3^- concentration was unevenly distributed, with the highest 77.3 − 82.9 μmol L^{-1} appearing in the inner part of the river mouth. It ranged from 15.6 to 74.2 μmol L^{-1} in the diluted area and was very low in the offshore area. The average PO_4^{3-} concentration was 0.80 μmol L^{-1} ± 0.44 μmol L^{-1}, with the maximum 1.9 μmol L^{-1} found at Station 40 and the minimum 0.21 μmol L^{-1} at Station 37.

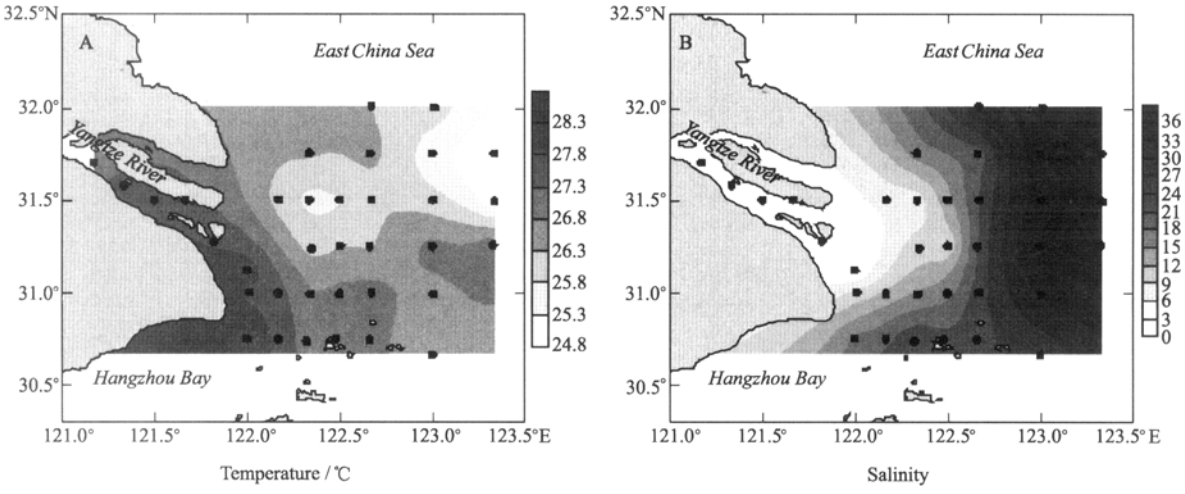

Fig.2 Surface temperature and salinity distributions of study area.

3.2 Species Composition

The composition of the phytoplankton community at the sampling stations was typical coastal regime. Phytoplankton assemblage was mainly dominated by Bacillariophyta. Pyrrophyta, Chlorophyta, Chrysophyta and Cyanophyta were much less. In the 130 phytoplankton water samples, 137 known species and 15 unknown species were identified. Of them 81 were found in Bacillariophyta, and 48 in Pyrrophyta, accounting for 59.1% and 35.0% (Table 1).

Table 1 Species composition of phytoplankton assemblage in the YRE and adjacent ECS†

Taxa	Taxa
Bacillariophyta	*Coscinodiscus jonesianus* Ostenfeld
Actinocyclus crassus v. Heurck	*Coscinodiscus marginatus* Ehrenberg
Actinocyclus octonarius Ehrenberg	*Coscinodiscus oculatus* (Fauv) Petit
Actinoptychus sp.	*Coscinodiscus oculus-iridis* Ehrenberg
Actinoptychus senarius (Ehrenberg) Ehrenberg	*Coscinodiscus radiatus* Ehrenberg
Actinoptychus splendens (Shadbolt) Ralfs	*Coscinodiscus wailesii* Gran et Angst
Actinoptychus trilingulatus Brightwell	*Coscinodiscus* spp.
Asteromphalus elegans Greville	*Cyclotella comta* (Ehrenberg) Kützing
Asteromphalus flabellatus Greville	*Cymbella* sp.
Asteroplanus karianus (Grunow) Gardner et Crawford	*Dactyliosolen fragilissimus* (Bergon) Hasle
Bacteriastrum hyalinum Lauder	*Diploneis bombus* Ehrenberg
Biddulphia granulata Roper	*Diploneis crabro* Ehrenberg
Bleakeleya notata (Grunow) Round	*Diploneis smithii* (Brébisson) Cleve
Cerataulina pelagica (Cleve) Hendey	*Ditylum brightwellii* (West) Grunow
Chaetoceros affinis Lauder	*Ditylum sol* Grunow
Chaetoceros atlanticus var. *skeleton* (Schütt) Hustedt	*Entomoneis alata* Ehrenberg
Chaetoceros curvisetus Cleve	*Fragilaria* sp.
Chaetoceros debilis Cleve	*Fragilaria capucina* (Desm.)
Chaetoceros didymus Ehrenberg	*Guinardia flaccida* (Castracane) Péragallo
Chaetoceros distans Cleve	*Guinardia striata* (Stolterfoth) Hasle
Chaetoceros eibenii Grunow	*Helicotheca tamesis* (Shrubsole) Ricard
Chaetoceros laciniosus Schütt	*Hemiaulux hauckii* Grunow
Chaetoceros laevis Leuduger-Fortmorel	*Hemiaulus membranacus* Cleve
Chaetoceros lorenzianus Grunow	*Hemiaulus sinensis* Greville
Chaetoceros vanheurcki Gran	*Lauderia annulata* Cleve
Chaetoceros spp.	*Leptocylindrus danicus* Cleve
Corethron hystrix Hensen	*Leptocylindrus mediterraneus* (Peragallo) Hasle
Coscinodiscus argus Ehrenberg	*Leptocylindrus minimus* Gran
Coscinodiscus curvatulus Grunow	*Licmophora abbreviata* Agardh
Coscinodiscus excentricus Ehrenberg	*Melosira granulata* (Ehrenberg) Ralfs

(*Continued on p.*126)

Table 1 (*Continued*)

Meuniera membranacea (Cleve) Silva
Navicula placentula (Ehrenberg) Grunow
Navicula rhynchocephala Kützing
Navicula sp.
Pseudo-nitzschia sp.
Odontella longicruis (Greville) Hoban
Odontella mobiliensis (Bailey) Grunow
Odontella regia (Schultze) Simonsen
Odontella sinensis (Greville) Grunow
Paralia sulcata (Ehrenberg) Cleve
Planktoniella blanda (Schmidt) Syvertsen & Hasle
Pleurosigma affine Grunow
Pleurosigma pelagicum Perag
Proboscia alata f. *gracillima* Cleve
Proboscia alata f. *indica* (Péragallo) Ostenfeld
Pseudo-nitzschia delicatissima (Cleve) Heiden
Pseudo-nitzschia pungens (Grunow ex Cleve) Hasle
Pseudosolenia calcar-avis (Schultze) Sundström
Rhizosolenia acuminata (Peragallo) Gran
Rhizosolenia robusta Norman
Rhizosolenia steigera Brightwell
Skeletonema costatum (Greville) Cleve
Surirella fastuosa Ehrenberg
Surirella sp.
Thalassionema frauenfeldii (Grunow) Hallegraeff
Thalassionema nitzschioides Grunow
Thalassiosira sp.
Thalassiosira leptopus (Grunow) Hasle & Fryxell
Thalassiosira nordenskiöldii Cleve
Thalassiosira rotula Meunier
Triceratium favus Ehrenberg

Pyrrophyta
Alexandrium sp.
Ceratium furca (Ehrenberg) Dujardin
Ceratium fusus (Ehrenberg) Dujardin
Ceratium intermedium (Jörgensen) Jörgensen
Ceratium kofoidii Jörgensen
Ceratium lineatum (Ehrenberg) Cleve
Ceratium macroceros (Ehrenberg) Cleve
Ceratium macroceros (Ehrenberg) var. *gallicum* (Kofoid) Jör-gensen
Ceratium tripos Nitsch
Dinophysis caudate Saville-Kent
Dinophysis fortii Pavillard
Diplopsalopsis orbicularis var. *ovata* (Paulsen) Meunier
Dissodinium lunula (Schütt) Schütt
Glenodinium danicum Paulsen
Goniodoma ostenfeldii Paulsen
Gonyaulax polygramma Stein
Gonyaulax spinifera (Clap. & Lach.) Diesing
Gonyaulax sp.
Gymnodinium lohmanni Paulsen
Gymnodinium viridescens Kofoid
Gymnodinium sp.
Gyrodinium spirale Bergh
Heterocapsa triqueta Stein
Noctiluca scintillans Surirey
Oxytoxum milneri Mürray Whitting
Oxytoxum scolopax Stein
Prorocentrum sp.
Prorocentrum dentatum Stein
Prorocentrum gracile Schütt
Prorocentrum micans Ehrenberg
Prorocentrum minimum (Pavillard) Schiller
Prorocentrum sigmoides Böhm
Prorocentrum triestinum Schiller
Protoperidinium bipes (Paulsen) Balech
Protoperidinium catenatum Levander
Protoperidinium cerasus Paulsen
Protoperidinium conicoides Paulsen
Protoperidinium conicum (Gran) Balech
Protoperidinium depressum (Bailey) Balech
Protoperidinium granii Ostenfeld
Protoperidinium oceanicum van Höffen
Protoperidinium oblongum (Aurivillius) Parke et Dodge
Protoperidinium ovum Schiller
Protoperidinium pallidum Ostenfeld
Protoperidinium pentagonum Gran
Protoperidinium puncutulatum Paulsen
Protoperidinium roseum Paulsen
Protoperidinium sphaeroidea Dangeard
Protoperidinium steinii Jörgensen
Protoperidinium subpyriforme Dangeard
Protoperidinium sp.
Pyrophacus steinii (Schiller) Wall & Dale
Scrippsiella trochoidea (Stein) Loeblich

Chlorophyta
Actinastrum sp.
Pediastrum simplex (Meyen) Lemmermanny
Scenedesmus quadricauda (Turpin) Brébisson
Scenedesmus sp.

Chrysophyta
Dictyocha fibula Ehrenberg
Dictyocha fibula var. *stapedia* (Haeckel) Lemmermann
Distephanus speculum (Ehrenberg) var. *octonarius* (Ehrenberg) Jörgensen
Emiliania huxleyi (Lohmann) Hay et Mohler
Gephyrocapsa oceanica Kamptner

Cyanophyta
Spirulina sp.
Trichodesmium thiebauti Gomont

Note: † For phytoplankton species nomenclature changes, refer to Sun and Liu (2002b).

3.3 Spatial Distribution of Phytoplankton

3.3.1 Horizontal distribution

The average cell abundance of surface water samples was 8.8×10^4 cells L^{-1}, with the maximum, 102.9×10^4 cells L^{-1}, found at Station 5 and the minimum, 0.2×10^4 cells L^{-1}, at Station 29. Distribution of phytoplankton cell abundance in surface water was shown in Fig.3. The dominant species in surface water were *Skeletonema costatum* and *Proboscia alata* f. *gracillima*, with cell abundance 225.7×10^4 cells L^{-1} and 43.6×10^4 cells L^{-1}, representing 73.5% and 14.2% of the total, respectively. The distribution of the Shannon-Wiener index and evenness in surface water were shown in Fig.4, with the maxima 4.06 (diversity index) and 0.86 (evenness) found at Station 32, and the minima 0.13 and 0.04 at Station 9. Chlorophyll *a* distribution in the summer of 2004 in YRE was consistent with that of cell abundance, with the highest two, 4.89 mg m^{-3} and 3.98 mg m^{-3}, appearing at Station 5 and Station 22 respectively.

3.3.2 Vertical distribution

Phytoplankton assemblage in the study area was mainly dominated by Bacillariophyta which had an evident preponderance over the others from the surface to the bottom in abundance (Fig.5). The suitable environmental condition produced by anthropogenic activity enhanced the growth and photosynthesis of phy-

toplankton and triggered the fast proliferation of dominant species. Supply of nitrate and phosphate was no longer the limitation on the growth of phytoplankton and thus caused the diatom bloom in the YRE.

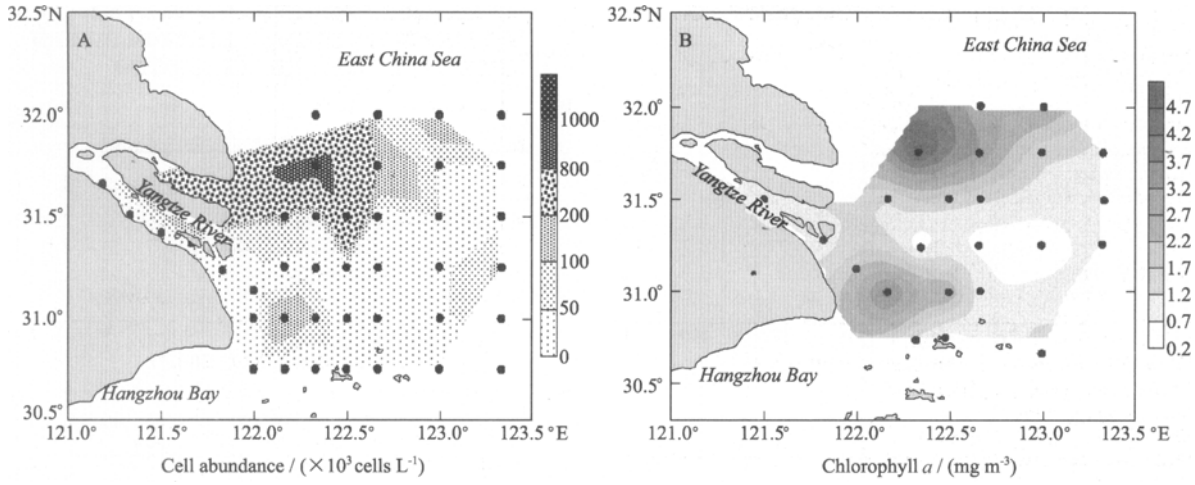

Fig.3 Cell abundance and chlorophyll *a* distributions of phytoplankton in surface water.

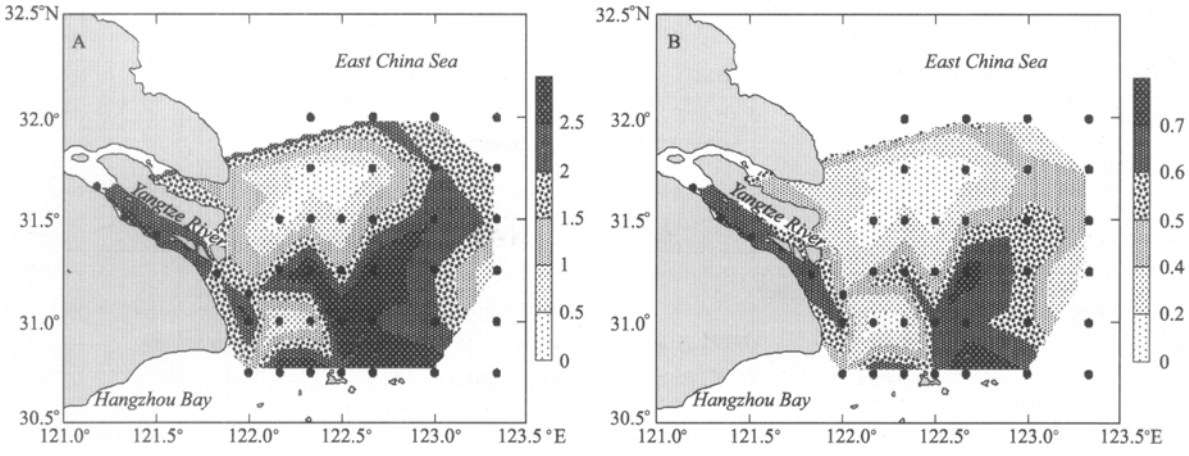

Fig.4 Shannon-Wiener index (A) and evenness (B) distributions of phytoplankton assemblage in surface water.

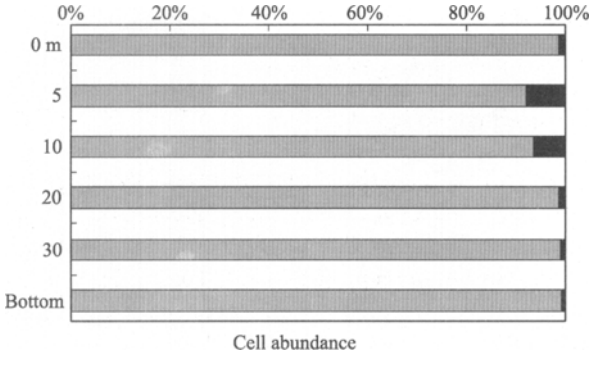

Fig.5 Relative cell abundances of Bacillariophyta and Pyrrophyta in water column. □ Bacillariophyta; ■ Pyrrophyta.

Phytoplankton cell abundance presented an obvious difference in different water column layers of Stations 33, 18 and 5, where obvious vertical dominant species variation was found also (Fig.6). The sharp variations of salinity and temperature in the vertical profile at these stations were the primary cause of stratification. However, no significant differences of vertical cell abundance distribution and dominant species variation were found at Station 8, where *P. alata* f. *gracillima* dominated the whole water column with an average cell abundance of 4.83×10^4 cells L^{-1}. At Stations 33 and 18, the maximum value of phytoplankton cell abundance appeared in the middle layer of water column 10 – 20 m below the surface. This might be caused by the excessive nutrient gradient in the middle water layer according to the different water masses movement. There was an obvious vertical transition of dominant species at Station 18, with the smaller cell species *S. costatum* in the upper water layer and the comparatively larger cell species *P. alata* f. *gracillima* from the depth of 10 m to bottom. Marvelous contrast in the vertical cell abundance distribution was found at Station 5. The primary production and biomass were much influenced by the co-effect of Yangtze River diluted water and continental coastal current. The cell abundance of dominant species *S. co-*

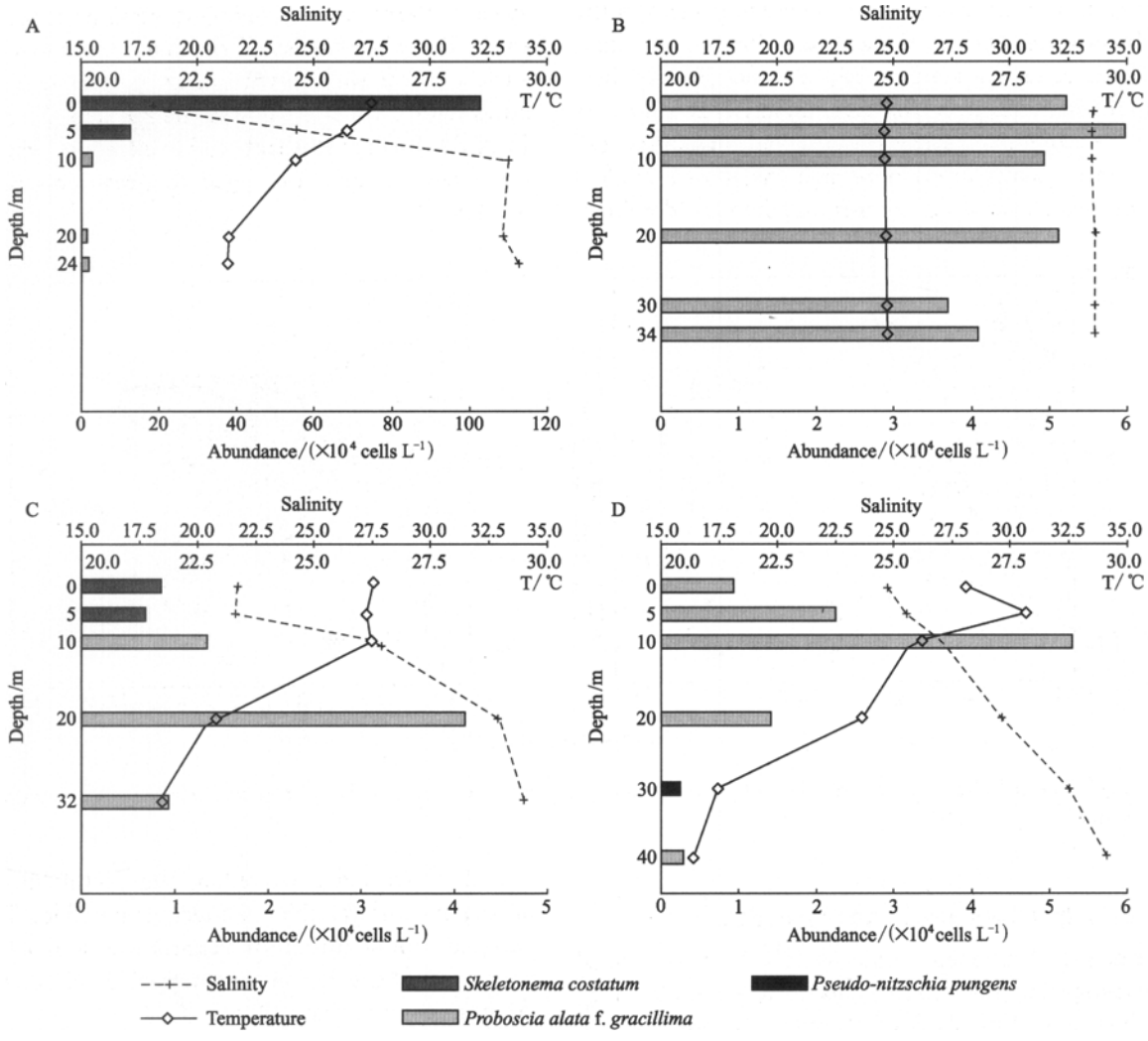

Fig.6 Vertical distributions of cell abundance, dominant species, salinity and temperature at Stations 5 (A), 8 (B), 18 (C) and 33 (D).

statum was 102.9×10^4 cells L^{-1} in surface water, contrasting to the 1.5×10^4 cells L^{-1} of *P. alata* f. *gracillima* near the bottom. The cell abundance in different water layers of Station 8 was unfluctuating, and the simplex dominant species was *P. alata* f. *gracillima* in the whole water column. A similar situation happened in the vertical distribution of salinity and temperature with no obvious changes at different water depths. Warm-oceanic species *Chaetoceros lorenzianus*, *Ditylum sol*, *Guinardia flaccida*, *Hemiaulus hauckii*, *Hemiaulus membranacus*, and *Rhizosolenia robusta* appeared at Stations 20, 26 and 33. The phytoplankton composition at these stations was influenced by the Taiwan Warm Current (Sun *et al.*, 2000a, b).

3.4 Dominant Species Analysis

The dominant species in the study area were *S. costatum* and *P. alata* f. *gracillima* with the dominance of 0.35 and 0.27, respectively. *S. costatum* is a low-salinity neritic species widely spreading near the

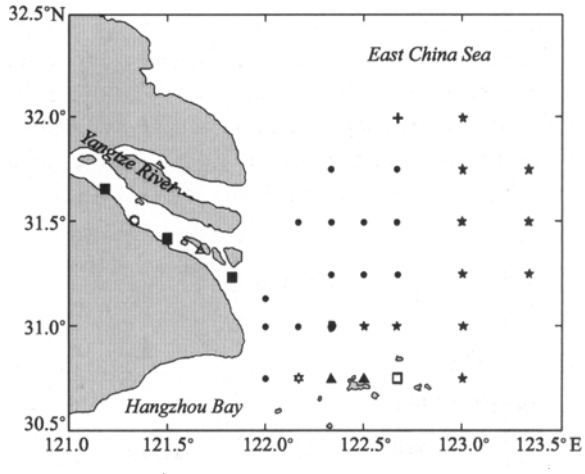

Fig.7 The distribution of dominant phytoplankton in surface water (Special symbols ○, ●, □, ■, △, ▲, +, ★ represent *Leptocylindrus danicus*, *S. costatum*, *Chaetoceros* spp., *Pedi. simplex*, *Melosira granulata*, *Pseudo-nitzschia pungens*, *Navicula* spp. and *P. alata* f. *gracillima*, respectively).

YRE with the optimum salinity *ca.* 19.2 (Li *et al.*,

2005). In the inner part of the Yangtze River Mouth, the fresh water species *Pediastrum simplex* dominated at the sampling stations 35, 37 and 39. At most sampling stations near the river mouth, *S. costatum* was the dominant species with the maximum cell abundance, while in offshore area the most abundant species was *P. alata* f. *gracillima*, and the dominant species altered among sampling stations from west to east. The distribution of dominant phytoplankton in surface water was shown in Fig.7. Abundance distributions of *P. alata* f. *gracillima* and *S. costatum* (Fig. 8) further illustrated the different water areas that were suitable for algae to grow and reproduce quickly.

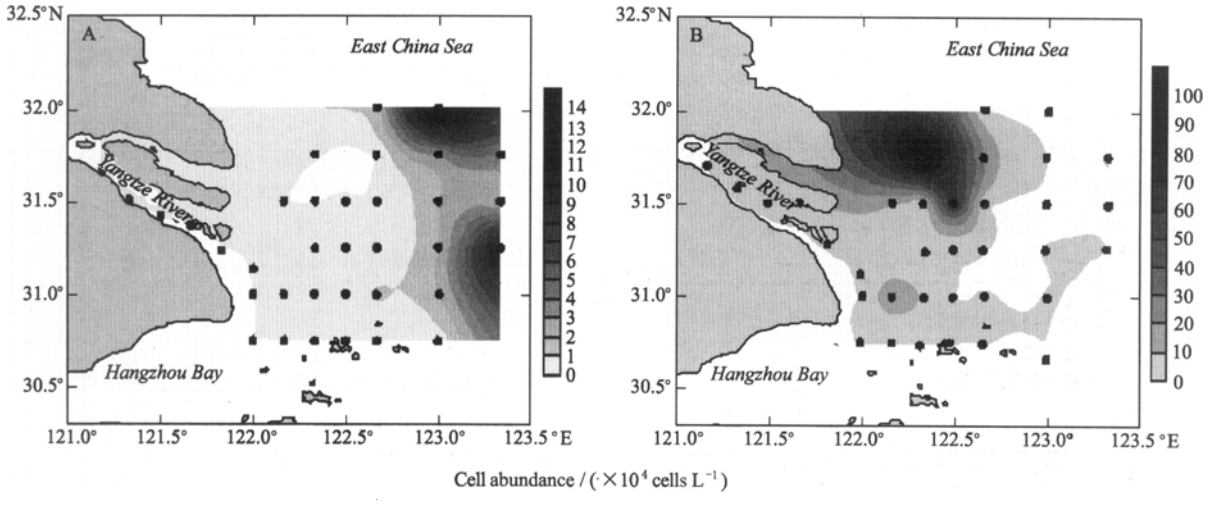

Fig.8 The cell abundance distributions of *Proboscia alata* f. *gracillima* (A) and *Skeletonema costatum* (B) in surface water.

3.5 Principal Component Analysis (PCA)

Principal Component Analysis (PCA) was applied to investigating the relationship between explanatory variables and phytoplankton growth. In order to determine the principal environmental factor with different explanatory variables, SPSS software package (version 12.0) was used. Eigenvalues and cumulate percentage variations could be calculated as well as the coefficient matrix, which thus were used to make up the formulas of the principal components. Factor analysis is often used in data reduction to identify a small number of factors that explain most of the variance observed in a much larger number of manifest variables. In the light of the PCA results, a few new variables can be abstracted and contain the useful information on the original variables as much as possible. The new variables can be interpreted synthetically in a scientific way and reflect the environmental conditions of the study area more truthfully.

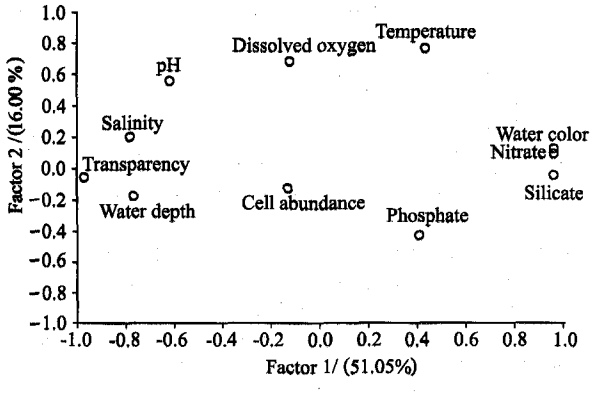

Fig.9 Loadings of environmental variables on the first two principal components extracted.

In order to summarize the weight of each parameter in an analysis of the dataset, PCA was applied for the reduction of dimensionality after the original environmental data were LG10-transformed and the original cell abundance data were SQRT-transformed. From the correlation matrix, two components were extracted with eigenvalues of 5.60 and 1.75 respectively, explaining 67.05% of the total variance.

The first principal component (PC1, explaining 51.05% of the total variance) was related to river discharge, as indicated by factor loadings, which was positive for inorganic nutrients and negative for salinity. Considering the first dimension, the contents of independent variables NO_3^- and SiO_3^{2-} contributed more to the loadings of factor 1 than PO_4^{3-} did. In contrast, salinity, transparency and water depth behaved adversely with the first component. Cell abundance was plotted in the intermediate position of the three crucial nutrient gradients and the salinity toward the direction of factor 1. This indicated that, in this costal system, the spatial distribution of nutrients was closely linked to river discharge. Consequently, low salinity generally corresponded to high nutrient concentrations, favoring the proliferation of small cell species like *S. costatum*.

The second component (PC2, explaining 16.00% of the total variance) was mainly due to variations in temperature and dissolved oxygen (DO). The pH lay in the middle area between salinity and DO, which contributed to both PC1 and PC2 with balanced influences.

4 Discussion

The YRE and its adjacent ECS is quite unstable and heterogeneous because of intense water exchange and advective processes. Due to high anthropogenic inputs, organic and inorgannic nutrients' concentrations are very high. Thus, interdisciplinary surveys were essential for the ecological study in this area.

Complex ecological processes and environmental factors influence the phytoplankton biomass and community structure in this region, including selective grazing (Sun *et al.*, 2003), competition, light availability (He *et al.*, 2001), trophic salts, temperature, salinity, turbidity (Xu *et al.*, 2004), and so on. Many of these factors have been examined in diverse experimental manipulations (*e.g.* mesocosms) that have provided valuable insight into the potential role of individual factors under controlled conditions (Li *et al.*, 2001). However, natural phytoplankton assemblage is exposed to the synergistic effects of all these known and unknown selective pressures. Primary production tends to be slightly limited in many estuaries, especially in the upper and fresh water reaches, where turbidity is usually the highest. Such is the case of the inner part of YRE, where light is the primary limiting factor because of the high turbidity and suspended solids. The latter can release absorbed nutrients into the seawater favoring eutrophication, but can weaken the penetration of sunlight. It does not favor photosynthesis. This has also been supported by the research in the estuarine area, where suspended and resuspended sediments caused by tidal disturbance from a high turbidity area result in a transparence of less than 3 m. The optimum balance of light and nutrients occurs at the middle region of the dilution zone which is about 100 km away from the river mouth and the east-side of Zhoushan Archipelago (Ning *et al.*, 2004). Light limitation resulting from suspended sediments is stronger than nutrient limitation in the estuarine ecosystem. This makes the primary production to be lower at the mouth area than at adjacent sea (He *et al.*, 2001). For this reason, the serious eutrophication produced by the huge amount of nutrient loaded via the Yangtze River is the main cause of phytoplankton bloom in the ECS.

The Shannon-Wiener index of phytoplankton assemblage presents a negative correlation with the cell abundance, since the dominant species reproduces fast, but it corresponds to the evenness distribution. The lowest value of Shannon-Wiener index (0.13) appeared at Station 9, which was contributed mainly by the small-cell species, *S. costatum*, with the cell abundance of 11.2×10^4 cells L^{-1}. Optimum salinity (14 – 23) of Yangtze River diluted water caused *S. costatum* to reproduce fast in an exponential pattern, leading to the bloom subsequently. This indicates that in the vicinity of river plume, nitrate, phosphate and silicate appear to be in excess, being not the limitation on phytoplankton growth. Similar results were also obtained in this area. *S. costatum* dominated in the vicinity of the river plume, and its distribution was consistent with the extension direction of the diluted water with a salinity of 10 – 20 (Gu *et al.*, 1995). Excessive multiplying of one species in a specific area is often accompanied with low Shannon-Wiener index of phytoplankton diversity.

Four typical sampling stations, 5, 8, 18 and 33, were chosen to analyze the vertical distributions of cell abundance and dominant species. The biomass and primary production were mainly influenced by the continental coastal current, mixed water of the Yellow Sea and ECS, Yangtze River diluted water and Taiwan Warm Current, respectively. The results showed that differences of vertical distribution were significant at Stations 5, 18 and 33, but no obvious vertical stratification was found at Station 8, where the abiotic environmental conditions, such as the salinity and temperature, were well-proportioned (Fig.6). *P. alata* f. *gracillima* was adapted to this specific niche substantially and became the dominant.

Given the correlations between the phytoplankton biomass and environmental factors such as nutrients, salinity, temperature, DO and pH, PCA analysis was used to summarize the weight of each parameter. According to the two dimensional plots of the variable loadings on the first two principal components, increased nutrient concentrations of NO_3^- and SiO_3^{2-} caused by the river loadings and the unstable temperature influenced by the heterogeneous water masses were primarily responsible for the phytoplankton growth in this area. However, the effect of PO_4^{3-} on phytoplankton growth is relatively lower than that of the nitrate and silicate mentioned above according to the contributions to the first component. Naturally, other variables also had integrated effects on the phytoplankton distribution which should not be neglected.

5 Summary

Results on the characteristics of the phytoplankton community structure in the study area indicated that cell abundance and Shannon-Wiener index were unevenly distributed. The highest value of cell abundance appeared in the diluted water area (Ⅱ). Pronounced stratification was found in the typical sam-

pling stations of 5, 18 and 33, showing the integrated influences of several water masses in YRE. With the rapid development of industry and agriculture in China, the discharge of sewage water and abundant nutrient gradients in the YRE caused serious eutrophication, favoring the phytoplankton bloom. This was also supported by the further considerations of the environmental variables, which made it clear that the nutrient loadings of the river discharge contributed more to the phytoplankton biomass dynamics and were mainly responsible for the alga blooms. Therefore, it is essential to conduct more field experiments including biological, chemical and physical surveys, and apply ecosystem dynamic model to further study.

Acknowledgements

This study was supported by the National Natural Science Foundation of China (Grant Nos. 50339040, 40306025) and the Chinese Academy of Sciences (No. KZCX3-SW-232). The authors are also very much indebted to the crews of the cruise.

References

Chen, Y., M. L. Shi, and Y. G. Zhao, 1989. *The Ecological and Environmental Atlas of the Three Gorges of the Yangtze*. Science Press, Beijing, 1-157.

Gu, X.G., Q.Yuan, J.W. Yang, and D. Hua, 1995. An ecological study on phytoplankton in frontal region of Yangtze estuarine area. *J. Fishery Sci. Chin.*, **2**(1): 1-15.

He, W. S., and J. J. Lu, 2001. Effects of high-density suspended sediments on primary production at the Yangtze Estuary. *Chin. J. Eco-Agricult.*, **9**(4): 24-27.

Li, J. T., W. H. Zhao, D. F. Yang, and J. T. Wang, 2005. Effect of turbid water in Yangtze Estuary on the growth of *S. costatum*. *Mar. Sci.*, **29**(1): 34-37.

Li, R. X., M.Y. Zhu, S. Chen, R.H.Lü, and B.H.Li, 2001. Responses of phytoplankton on phosphate enrichment in mesocosms. *Acta Ecologica Sinica*, **21**(4): 603-607.

Ning, X. R., V. Daniel, Z. Liu, and Z. Liu, 1988. Standing stock and production of phytoplankton in the estuary of the Yangtze River and the adjacent East China Sea. *Mar. Ecol. Prog. Ser.*, **49**(10): 141-150.

Ning, X. R., J. X. Shi, Y.M. Cai, and C. G. Liu, 2004. Biological productivity front in the Yangtze Estuary and the Hangzhou Bay and its ecological effects. *Acta Oceanologica Sinica*, **26**(6): 96-106.

Pielou, E. C., 1969. *An Introduction to Mathematical Ecology*. Wiley-Interscience, New York, 1-286.

Pu, X. M., Y. L. Wu, and Y. S. Zhang, 2000. Nutrient limitation of phytoplankton in the Yangtze Estuary Ⅰ: Condition of nutrient limitation in autumn. *Acta Oceanologica Sinica*, **22**(4): 60-66.

Pu, X. M., Y. L. Wu, and Y. S. Zhang, 2001. Nutrient limitation of phytoplankton in the Yangtze Estuary Ⅱ: Condition of nutrient limitation in spring. *Acta Oceanologica Sinica*, **23**(3): 57-65.

Shannon, C. E., and W. Wiener, 1949. *The Mathematical Theory of Communication*. University of Illinois Press, Urbana IL, 1-117.

Shen, Z. L., J. P. Lu, X. J. Liu, and H. X. Diao, 1992. Distribution feature of nutrient in the Yangtze Estuary and impact of the Three Gorges Dam on it. *Marina Studia Sinica*, **33**: 109-129.

Sun, J., D. Y. Liu, Y. Yin, X. Y. Chai, and S. B. Qian, 2000a. Standing crop distribution and species composition of phytoplankton near Ryukyu islands water and its correlation with water mass in summer of 1997. In: *Proceedings of China-Japan Joint Symposium on CSSCS*. China Ocean Press, Beijing, 191-203.

Sun, J., D. Y. Liu, and S. B. Qian, 2000b. Planktonic diatoms in Ryukyu-gunto and its adjacent waters: Species composition and their abundance distribution in the summer of 1997. in: *Oceanography in China*. China Ocean Press, Beijing, 158-165.

Sun, J., D. Y. Liu, Z. L. Wang, X. Y. Shi, R. X. Li, *et al.*, 2003. Microzooplankton herbivory during red tide-frequent-occurrence period in spring in the East China Sea. *Chin. J. Appl. Ecol.*, **14**(7): 1073-1080.

Sun, J., D.Y. Liu, and S.B.Qian, 2002a. A quantative research and analysis method for marine phytoplankton: An introduction to Utermöhl method and its modification. *J. Oceanogr. Huanghai Bohai Seas*, **20**(2): 105-112.

Sun, J., and D.Y. Liu, 2002b. The preliminary notion on nomenclature of common phytoplankton in China seas water. *Oceanologia et Limnologia Sinica*, **33**(3): 271-286.

Tomas, C. R., 1997. *Identifying Marine Phytoplankton*. Academic Press, San Diego, 1-858.

Utermöhl, H., 1958. Zur Vervolkommung der quantitativen Phytoplankton-Methodik. *Mitt. Int. Ver. Theor. Angew. Limnol.*, **9**: 1-38.

Xu, Z. L., X. Q. Shen, and Y.Q. Chen, 2004. Effect of the suspended sands on growth of *Chaetoceros muelleri* in Yangtze Estuary. *Mar. Environ. Sci.*, **23**(4): 28-30.

Yamaji, I., 1991. *Illustrations of the Marine Plankton of Japan*. Hoikusha Publishing Co., Ltd., Osaka, 1-538.

Zhao, W. H., J. T. Li, and J. T. Wang, 2004. Study on nutrient limitation of phytoplankton in field experiment of Yangtze Estuary in summer. *Mar. Environ. Sci.*, **23**(4): 1-5.

Zhu, J. R., J. H. Wang, and H. T. Shen, 2005. Observation and analysis of the diluted water and red tide in the sea off the Yangtze mouth in middle and late June 2003. *Chin. Sci. Bull.*, **50**(3): 240-247.